Nano-Bio-Chemical Braille for Cells: The Regulation of Stem Cell Responses using Bi-Functional Surfaces

Wojciech Chrzanowski, Jae Ho Lee, Alexey Kondyurin, Megan S. Lord, Jun-Hyeog Jang, Hae-Won Kim, and Marcela M. M. Bilek**

Insufficient integration with local host tissues is a significant problem that adversely affects the performance of implanted biomedical devices. Poor tissue integration leaves patients susceptible to complications associated with adverse foreign body reactions and infections that typically mandate expensive and elevated-risk revision surgery. The aging population and growing incidence of medical implants makes the development of bio-functional implant surfaces a high priority research imperative. Here multifunctional surfaces are reported that are capable of regulating cell adhesion and triggering cell differentiation to facilitate osseointegration of implantable devices. The approach described is universal, cost- and time-effective. It relies on a unique combination of two advances: i) a reactive interface provided by a plasma activated coating (PAC) that covalently immobilises bioactive molecules with significantly higher efficiency than conventional technologies, and ii) multifunctional molecules (bi-functional fusion-proteins) that regulate multiple cellular responses. Covalent linking of the molecules, their high density, and desired orientation are demonstrated. The effectiveness of these functional interfaces to regulate mesenchymal stem cell attachment and differentiation is confirmed suggesting the ability to regulate osseointegration. This method is a leap forward in the fabrication of truly biofunctional materials tailored for particular applications.

1. Introduction

A rapidly aging population has driven the increasing demand for implantable devices, such as orthopaedic implants, pacemakers, or cochlear implants. The number of orthopaedic implants alone inserted annually worldwide is estimated at 3.7 million[1] and it is steadily increasing at a rate of 8% per annum.[2–4] The implantation of devices into tissues induces foreign body reactions which often lead to the development of fibrous capsules that enclose the device separating it from the body.[2–4] Such reactions are detrimental to the function of the implant, reduce its lifetime, and often necessitate revision surgery.[2,5,6] In fact, Ratner[1–4,7,8] argues that essentially all materials used in medicine today trigger such a reaction upon implantation, which reduces implant function and precipitates the failure of the medical devices.[8–12] Subsequently, foreign body reactions (FBRs) can lead to implant removal or replacement entailing massive trauma for patients, and generating considerable additional costs.[5,13] The percentage of implants that require removal or revision vary between sites of implantation, reaching 17% for joint replacements. These incidents are predominately caused by a lack of cues that are capable of regulating cell attachment, differentiation and cell functionality on implant surfaces.[1,5,7,11,14–16]

Surface topography, chemistry and stiffness are three of the key factors that have been found to regulate cell

Dr. W. Chrzanowski
Faculty of Pharmacy
Pharmacy and Bank Building A15
University of Sydney
NSW 2006, Australia

Dr. A. Kondyurin, Prof. M. M. M. Bilek
School of Physics
University of Sydney
NSW 2006, Australia
E-mail: marcela.bilek@sydney.edu.au

Dr. J. H. Lee, Prof. H.-W. Kim
Institute of Tissue Regenerative Engineering (ITREN)
Dankook University
Cheonan 330–715, Republic of Korea
E-mail: kimhw@dku.edu

Dr. W. Chrzanowski, Prof. H.-W. Kim
Department of Nanobiomedical Science and BK21 PLUS NBM Global Research Center for Regenerative Medicine
Dankook University
Cheonan 330–715, Republic of Korea

DOI: 10.1002/adfm.201401696

Dr. M. S. Lord
Graduate School of Biomedical Engineering
University of New South Wales
Sydney, NSW 2052, Australia

Prof. J.-H. Jang
Department of Biochemistry
Inha University School of Medicine
Incheon 400–712, Korea

Prof. H.-W. Kim
Department of Biomaterials Science
College of Dentistry
Dankook University
Cheonan 330–715, Republic of Korea

responses.[7,10,14,16–21] It has been reported that cell modulation can be achieved using topographically modified substrates. Ground-breaking research by Dalby has demonstrated that using a specific arrangement of nanotopographical cues it was possible to "switch-on" osteoblastic differentiation of mesenchymal stem cells.[14,16,22–27] However, topographical approaches present some limitations in respect to their clinical translation. Furthermore, the interaction of proteins/biomolecules from body fluids with the topographically modified substrate and the effects of the topographies on protein conformation and subsequently on cellular responses have not been well described. It is, however, well established that cell adhesion is mediated by interactions with pre-adsorbed proteins which, if they have the correct geometry and chemistry, can act as anchors for cell adhesion,[28–30] and then signal into cells through their membrane receptors.

Integrin binding sites of cells interact with specific peptides or regions within proteins (such as the tripeptide arginine-glycine-aspartic acid, RGD).[27–29] When these peptides are exposed and available, they actively promote cellular attachment and spreading.[17,18,20,31] Surface chemistry and geometry have been shown to play fundamental roles in protein adsorption and binding to surfaces, and they can introduce conformational changes to the protein structure. Fibrinogen becomes denaturated when it binds to a surface with high curvature (curvature less than 30 nm) and protein preferential orientation (side-on or end-on) is related to the surface topography.[32,33] For the development of functional surfaces it is essential to control the binding of protein without introducing structural disorders. Current approaches of protein binding to metal implants using chemical linkers or adsorption have severe limitations including: the requirement for expensive specialised chemical linkers and solvents, incomplete or side reactions, changes to protein structure due to chemical binding; or, in the case of physical adsorption, poor attachment of the protein to the surface as well as structural changes.

It is well established that cells communicate with the surface via an adsorbed protein layer that forms on the surface immediately after implantation and it is these protein structures that regulate specific cellular responses.[17,34,35] So far chemical functionalisation of surfaces and the binding of proteins using chemical linkers has achieved some success,[2,30,32,33,36–38] however fundamental questions remain such as whether the chemical binding impacts on proteins' conformation and efficacy, and whether an optimal density of the proteins can be achieved. Surface immobilisation of proteins using chemical linkers is also not easily transferred to applications on practical implants. There are limited data on activity of chemically immobilised molecules and the majority of approaches consider only single molecule coverage which provides limited functionality.[17,39–42] For multifaceted stimulation it would be logical to use different classes of molecules tethered to the surface, although difficulties in controlling immobilisation (adhesion), densities, distribution and activity of multiple molecules including proteins have been reported.[43–45] Taken together, these findings raise the tantalising possibility that by fabricating surfaces with immobilised multifunctional molecules that have exposed integrin binding sites (i.e., cell-adhesive RGD binding sites) and at the same time show osteogenic potential, both cell adhesion and cell differentiation could be significantly improved and appropriately regulated. This concept presents a significant advantage where a single, yet multifunctional, molecule immobilised on the surface would provide enhanced cell adhesion, regulate differentiation and mineralisation, yielding desired integration of the orthopaedic implant. The development of a simple method that allows the immobilisation of biomolecules on the surfaces without introducing conformational changes to the attached biomolecules and the development of novel bifunctional fusion molecules that have the capability to regulate cell responses has so far proved elusive. The cumulative effects of two separate active sites within one molecule tethered to the surface can provide highly desired clinically relevant regulation of progenitor and stem cells, applicable to various applications including the expansion of stem cells.

In the study described here, we demonstrate a novel bifunctional fusion-protein immobilised on a surface using a new generation of active interface for use on orthopaedic implants. This bioactive surface was able to effectively regulate mesenchymal stem cell adhesion and differentiation. In traditional approaches only a single type of response is promoted and multifunctionality is a significant advantage of the approach presented. Our fusion-protein combines the cell-binding site of fibronectin (the RGD sequence, FN9–10) with osteocalcin (OCN).

Osteocalcin (OCN) is one of very few osteoblast-specific proteins and it is a marker of osteogenesis.[46–48] OCN has several features of a hormone, which is a cell-specific molecule, synthesised as a pre-pro molecule (protein precursor secreted by cells) and secreted into general circulation. Furthermore, OCN mediates the metabolic functions of osteoblasts.[49] It undergoes an unusual post-translational modification whereby glutamic acid residues are carboxylated to form γ-carboxyglutamic acid (Gla) residues, hence its other name, bone Gla protein. This modification confers to the protein a high affinity for mineral ions, and thus OCN is recognised as a key protein involved in the matrix maturation and mineralisation processes of bone.[46–48,50,51] As it is the main circulating molecule to regulate bone metabolic functions,[52] we hypothesise that immobilised osteocalcin on the surface of bone implants has the potential to stimulate osteogenesis and cellular mineralisation. It is also worth noting that current literature reports that OCN does not inhibit the mineralisation of ECM,[48] and this may not be the case with supplementation by other proteins expressed by cells.

The protein is immobilised on the surface via active radical-rich interfaces, capable of linker-free immobilisation of biomolecules.[39] This active interface, obtained via pre-treatment with ion implantation, makes the process of surface functionalisation simple and allows the effective, well controlled covalent tethering of biomolecules to the surface without introducing significant changes to the biomolecules' conformations.[53]

The combination of both advances i) fusion-protein (FN-OCN) that was immobilised using our ii) active interface (plasma activated coating, PAC), creates a truly multifunctional interface that provides unprecedented control of cellular responses.

We hypothesize that such nanobiointerfaces will greatly enhance the integration of devices in the body. This is a cost-effective and single-step surface functionalisation technology

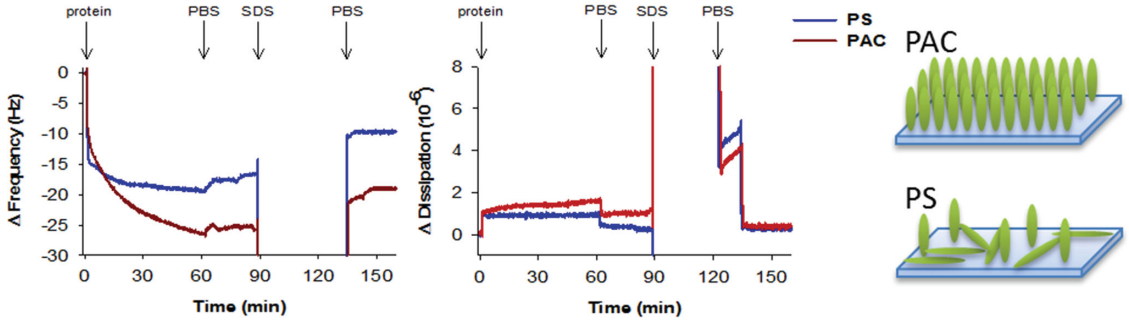

Figure 1. Comparison of frequency and dissipation measurements for osteocalcin/fibronectin combination protein exposed PS and PAC surfaces determined by QCM-D. Significantly higher frequency changes, associated with the amount and the thickness of the adsorbed layer, were observed for PAC samples indicating greater amount of surface immobilised protein. Similarly dissipation energy changes suggest greater thickness and end-on orientation of the adsorbed proteins to the surface. Furthermore PBS and SDS washes reduced frequency and dissipation changes, indicating some detachment of protein. The ion implanted PAC surfaces immobilised over 2× more protein and retained more protein than the PS surfaces. Dissipation data suggests formation of a monolayer with the preferred end-on orientation of the proteins.

that can be employed to regulate the integration of a wide range of medical devices including those with complex geometry. A further attractive feature of this technology is that after the plasma ion treatment the implant is sterile. Major advances demonstrated in our study are protein binding to the implant surface, without using specialised chemical linkers, and that the plasma activated interface with covalently bound bi-functional proteins presents a biochemically active surface capable of regulating cell responses.

2. Results and Discussion

Covalent binding of the fusion-protein was achieved via a radical rich polymer interface. Samples made of nickel-titanium, which is used for implantable devices, and for which integration within the body is one of the major issues was used in the study. This material is characterised also by limited bioactivity in the body, which was a major incentive for using it to demonstrate the strength of our approach and its applicability to non-bioactive materials. To create active interfaces, samples were polymer coated with polystyrene (PS), which acts as a precursor to form the reactive radical-rich interface—plasma activated coating (PAC). The thickness of the spun PS coating measured with ellipsometry was 9.00 ± 0.05 nm. This polymer film was then activated using energetic ion bombardment (ion implantation), which disrupts the primary bonds of the polymer and results in the formation of a carbonised interface that contains highly reactive radical species with unpaired electrons.[53,54] The radicals are stabilised by delocalisation on π-electron clouds of the condensed aromatic structures. The stability increases with larger conjugated areas in the aromatic structure. Due to the chemical activity that they bring to the surface, the unpaired electrons typically react with oxygen in the environment[55] and create a negative potential on the surface, that generates a double layer in solution and attracts the protein molecules to the surface. The radicals in the interface also facilitate the covalent binding of the biomolecules without the need for any additional linkers.[39] It is believed that the reactive radicals immobilise biomolecules through the substitution of mobile hydrogen atoms bonded to carbon, nitrogen, sulfur or oxygen atoms in amino acids on the outer surface of the protein molecule. At the same time, the radicals and surface oxygen groups interact with water molecules due to strong hydrogen bonds providing a hydrophilic surface. It is believed that an adsorbed water layer prevents direct physical contact of the protein molecule with the surface creating a water shell around the protein and maintaining the natural conformation of the protein molecule despite the covalent bonding with the surface.[56]

To functionalise surfaces a solution of proteins was applied at the concentration of 20 µg/mL and surfaces were incubated for 6 h. If all the protein in the solution applied were immobilised, it would give a protein loading of 4 µg/cm^2. As a control unmodified (non-activated) PS coated surfaces were used. To test both cell-binding efficacy and differentiation regulation capability, surfaces were incubated with i) fibronectin only (PAC-FN) and ii) the fusion-protein combining the fibronectin RGD containing domain and osteocalcin (PAC-FN-OCN).

The study of protein adsorption kinetics for the fibronectin-osteocalcin (FN-OCN) system showed a significantly increased (over a factor of two) amount of protein on the PAC (activated interfaces), when compared with non-activated coatings. This is consistent with previous studies of single protein and enzyme attachment to similar surfaces.[17,57] Importantly, the evidence from the measurements of dissipation energy (quartz crystal microbalance – QCM-D, **Figure 1**) during protein immobilisation on PAC indicated the desired end-on orientation of the protein. These results suggest that the active sites of the proteins are exposed (**Figure 2**). In contrast, on the non-activated coating (PS) dissipation times were very short, which suggests much smaller thickness, surface density and quite likely an undesired side-on orientation of the protein.

When proteins approach the surface, interactions with the surface can guide the formation of stable and correctly (end-on) oriented protein layers.[32,33] The ability of the surface to immobilise proteins in the correct orientation and density is critical to achieve desired responses of cells and tissues. Once the first layer is immobilised there will always be some interactions of the proteins that are present in the surrounding environment, with the proteins that are already immobilised. Consequently it is possible to form a multilayer in cases where the proteins in the environment self-assemble or aggregate with those on

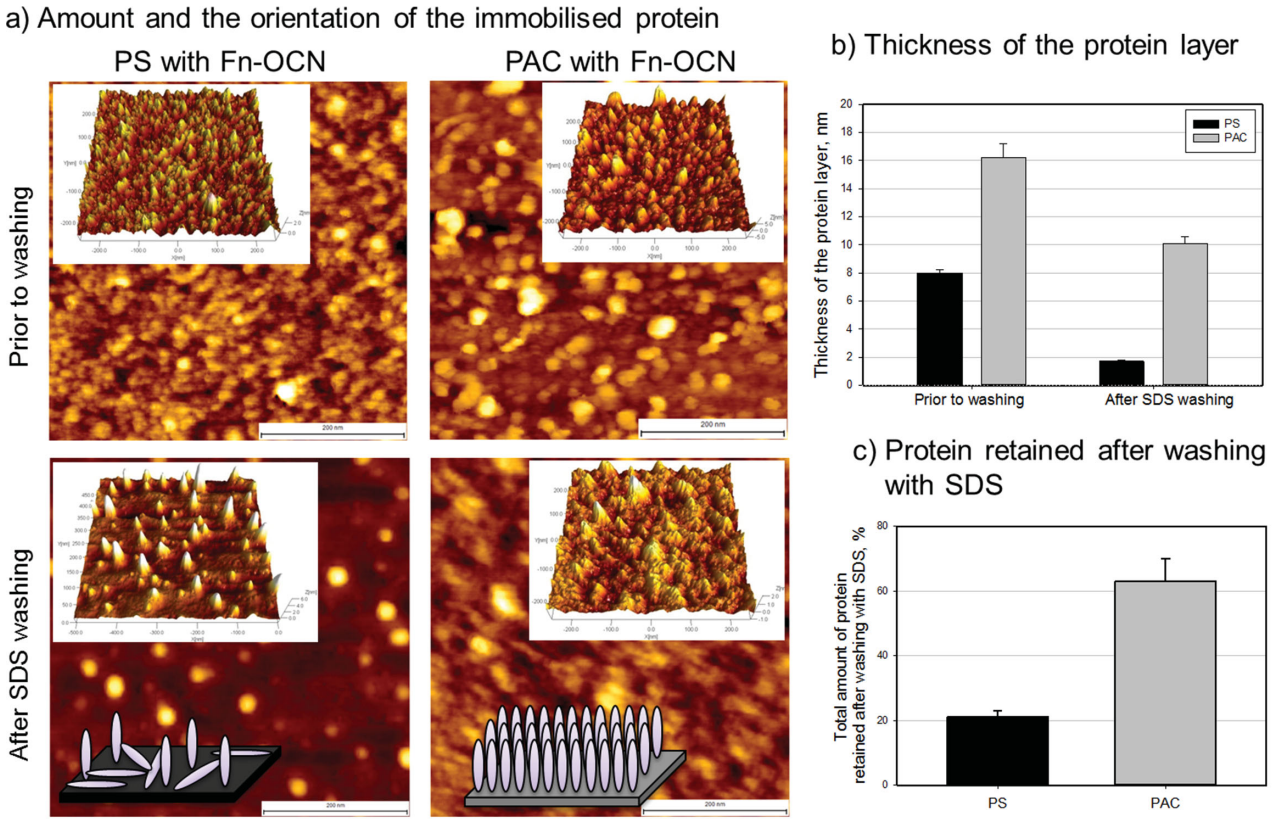

Figure 2. Qualitative and quantitative assessment of the immobilised fusion protein on the plasma activated (PAC) and non-activated polystyrene (PS) coated silicon before and after washing with SDS. a) Topographical images demonstrate a high density of proteins on the PAC surfaces, while a much lesser amount is observed on the non-activated PS surfaces. b,c) After washing the samples with SDS only small decreases (small changes to the topography) were observed for the ion-implanted surfaces, suggesting covalent attachment of the proteins. For PS surfaces very significant changes to the topography were observed and a significant amount of the protein was removed by SDS washing (b,c).

the surface. However, in cases where the conformation of the immobilised protein is not significantly modified adhesion forces between these extra layers are weak and simple washing with buffer solution is capable of disrupting them. Our measurements of the protein adsorption (QCM-D) showed that the mass of protein increased and then plateaued, suggesting very limited interactions between proteins beyond the initial layer immobilised to the surface. After washing the mass slightly decreased, which indicates the removal of loosely attached proteins. Based on the adsorption and dissipation energy measurements, which were conducted after washing with PBS, it is suggested that the end-on orientation of the protein on PAC surfaces is likely. These results are in agreement with molecular force probing, which was conducted after washing samples with PBS, and which demonstrated a high density of active sites present on the sample. Based on the mass of protein covalently attached (1.12 μg/cm^2 measured with QCM-D after washing with SDS) and the molecular weight of the protein (41 kDa), the area per immobilised protein molecule can be calculated as 6 nm^2. This is consistent with a dense monolayer attached in the end-on orientation.

The rate of adsorption was significantly greater on the PAC and it corresponded well with the mass of proteins adsorbed to the surface (Figure 2). Based on QCM-D analyses, the masses of combined protein on PS and PAC were 900 and 1800 ng/cm^2 respectively (Figure 2). Results showed that approximately two times more protein adsorbed on the PAC (**Table 1**), and the large dissipation time constants suggested an end-on orientation. The QCM-D masses report the mass associated with bound protein, so the surface mass densities reported by QCM-D can be 4–8 times higher than measurements with optical techniques which do not incorporate bound water shells.[58] We have previously reported fibronectin bound onto oxidised polystyrene, regarded as a highly reactive

Table 1. Quantification of fibronectin-osteocalcin combination protein on PS and PAC analysed by QCM-D. Data presented as the mass of adsorbed protein after coating with protein and PBS rinsing as well as after protein coating and rinsing with PBS, SDS and PBS again. The percentage of the originally adsorbed protein retained on the surface after all rinses was also calculated. The data is presented as mean ± standard error ($n = 2$)

	Protein thickness [ng]		Protein retained on surfaces at the end of the experiment [%]
	After protein adsorption and PBS rinsing	After protein adsorption, PBS, SDS and PBS rinsing	
PS	880.0 ± 22.2	187 ± 10.1	21 ± 2
PAC	1782 ± 110.0	1111 ± 55	63 ± 7

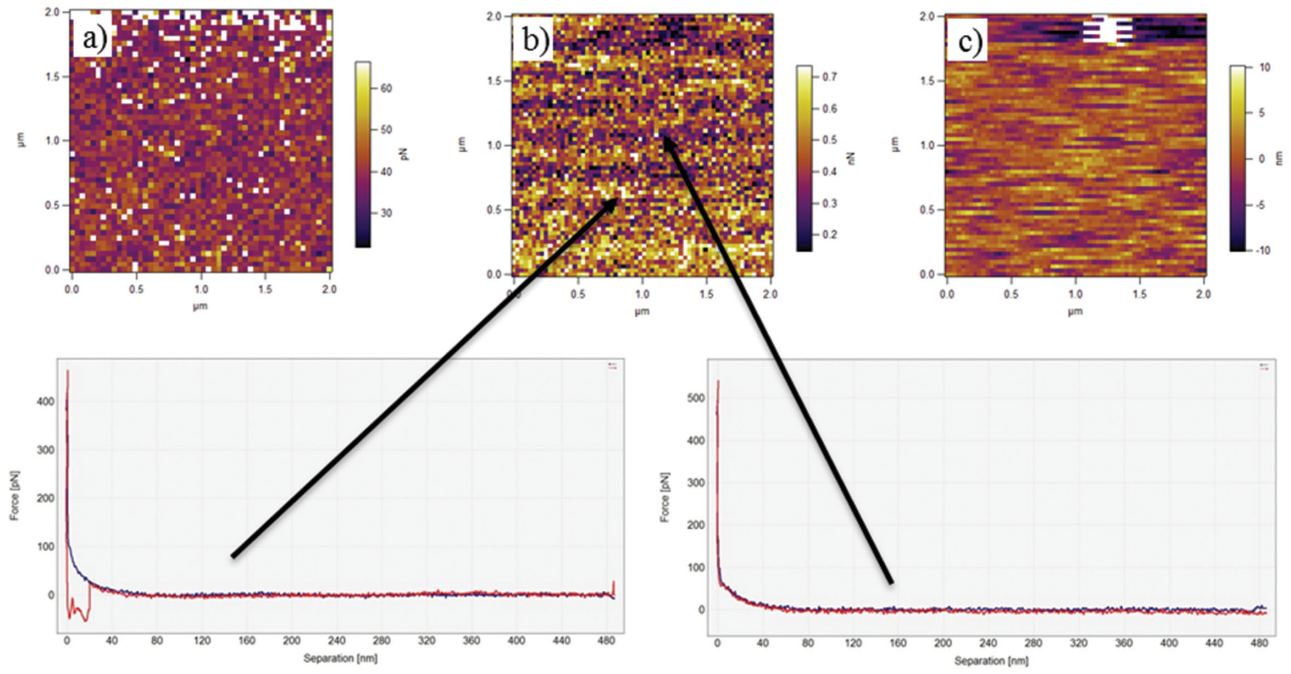

Figure 3. Distribution of proteins on the surfaces obtained by molecular probe imaging using AFM; map of adhesion forces between functionalised tip and substrates with immobilised fusion-proteins for: a) untreated polystyrene and b) PAC; c) topography for PAC that shows corresponding high image for the adhesion force map (b). The uniform distribution of the protein on the PS coated samples with very low adhesion force measurements suggests weak adhesion of the protein to the substrate. The PAC, in contrast, showed uniform regions of protein with occasional agglomerates. Adhesion forces were significantly greater than observed for untreated samples. The agglomerates showed low adhesion to the anti-osteocalcin coated tip suggesting that agglomerates were composed of end-exposed fibronectin.

surface, to be around 920 ± 100 ng/cm^2,[18,59] which is comparable to the amount of fibronectin adsorbed onto non-ion-implanted PS in this study. This finding demonstrates the superior properties of our new PAC interfaces to immobilise protein. The PAC active surfaces appeared to be at least two times more effective than untreated or previously reported oxidised polystyrene. The dry protein mass of fibronectin adsorbed in a monolayer is between 300 ng/cm^2 (pure relaxed side-on orientation) to 2000 ng/cm^2 (for the completely end on orientation). Cumulative analysis of frequency and dissipation energy changes (Figure 1) after washing and rinsing with SDS and PBS, which are effective to remove non-covalently attached molecules, suggested clearly that PAC surfaces more effectively immobilised proteins and that the proteins were adsorbed in sub-monolayer levels on PS, while they formed end-on monolayers on the PAC.

In the assessment of protein immobilisation (QCM-D), after incubation with fibronectin- osteocalcin combination protein, samples were washed with SDS to determine the extent of irreversible binding. After treatment of PAC with SDS approximately 63% of the initially adsorbed protein was retained, or 1111 ng/cm^2, while the PS surfaces maintained only 187 ng/cm^2.

The presence of proteins and the formation of a monolayer was confirmed with atomic force microscopy; surface topography was examined before and after protein immobilisation (Figure 2). The results show that the proteins formed a uniform layer when fibronectin (FN9–10) alone was used. When the FN-OCN fusion-protein was immobilised some regions with more agglomerated structures were observed (Figure 2). This phenomenon can be explained when we compare the sizes of these proteins: FN has a length of 15.5 ±1.3 nm and a width of 8.8 ± 1.7 nm, and native OCN has an average width of 1.5 nm in biological fluids.[60,61]

To confirm the distribution of the proteins we conducted molecular force probing (adhesion forces/energy) using a functionalised atomic force microscope tip. Tips were functionalised with antibodies (anti-osteocalcin) and force-volume measurements were conducted. Based on adhesion forces it was possible to locate proteins which have exposed motifs to which the tip-immobilised antibodies bind specifically. Nanoscale regions of high adhesion force suggest the location of osteocalcin. Typical maximum force values for PAC samples were 700 pN to 1 nN whereas for PS samples maximum recorded values were of below 70 pN. According to force values observed the PAC interfaces have uniformly distributed osteocalcin amongst regions with negligible adhesion that suggested fibronectin (**Figure 3**). The agglomerated regions (top part of the image – white zone Figure 3c), seen on the topographical images, showed very little adhesion, which suggests that OCN was hidden inside the aggregates.

When we conducted molecular probe imaging on the non-ion-activated surfaces we observed a uniform distribution of the protein but the forces of adhesion were very low (below 70 pN). In addition, at the beginning of the experiment (top part of the images – Figure 3a) the largest relative adhesion forces were measured. This result suggests that the adhesion forces between the protein and the surface were very low. It is most

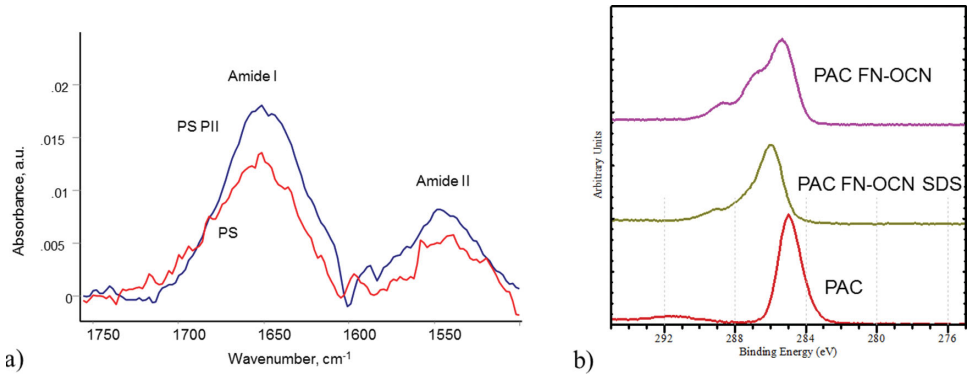

Figure 4. FTIR-ATR and XPS spectra of fusion-protein attached to the non-ion-activated (PS) and plasma activated coating (PAC): a) FTIR-ATR shows the presence of well pronounced Amide I and II for both plasma activated (PAC) and control polystyrene (PS) samples, confirming that there is more protein attached to the PAC surface than to the non-activated PS (see also QCM-D data); b) detailed XPS spectra (C1s) for PAC show an increase in the contribution of carbon in C-O and C = O structures at higher binding energy after immobilisation of the protein; the contribution of carbon with greater binding energy (E_b = 287.5eV) detected on samples with proteins before and after washing with SDS suggests a significant amount of protein immobilised on the PAC surface.

likely that the adhesion of the protein to the anti-body functionalised AFM tip was larger than the adhesion of the proteins to the surface and the probe pulled the protein off the surface. Once this occurred the tip became gradually blocked, unable to detect any further specific interactions with exposed motifs of osteocalcin and hence all subsequent interaction forces are lower.

We next sought to determine the nature of the bonding of protein to the ion-activated surface. We used a technique that relies on rigorous detergent washing to disrupt physical interactions as previously described in the literature.[62,63] In a rigorous SDS detergent wash, the unbound or physisorbed protein is washed away because the SDS detergent disrupts weak Van der Walls and electrostatic interactions. Covalently bonded protein is denatured by the detergent but remains on the surface because covalent bonds are left intact. Removal of the majority of the protein layer from the non-ion-activated surfaces was confirmed by both QCM-D and AFM measurements (Figure 3). QCM-D quantitative measurements demonstrated that a large proportion of protein was removed by an SDS rinse from non-ion-activated polymer coated samples (PS); only around 20% was present on the surface after the SDS rinse. In contrast for ion-activated PAC surfaces, over 60% of the protein remained on the surface (Table 1). This result corresponded very well with measurements of the immobilised layer thickness and dissipation energy, which indicated that proteins were robustly immobilised as a monolayer with desired end-on orientation on the PAC surface.

Further these results were confirmed by AFM observations and by XPS analysis. XPS examined changes to the oxygen, carbon, and nitrogen peaks. Deconvolution of the peaks was employed to observe the intensity of signals from bonding states present in proteins (at binding energies of E_b^C = 283 eV, E_b^O = 532 eV, E_b^N = 401 eV) and relative changes in the intensities of these contributions give an indication of changes in the amount of protein present. This time the washing procedure applied was much more rigorous (SDS, 10 min, 100 °C) than could be achieved in the QCM-D system due to temperature limitations. Despite the very hash washing conditions, the presence of a dense protein layer was confirmed on the ion-activated surfaces when using both fibronectin and fusion-protein (Figure 2). There were no significant differences in topography and morphology before and after washing for PAC surfaces and negligible changes to the XPS spectra were observed (**Figure 4**, and Supporting Information Figure S1). Only a small fraction of residual protein was observed on PS surfaces and the signals from protein relevant bonding states of C, N, and O were significantly reduced after washing with SDS. This demonstrates the effectiveness of the PAC interfaces to covalently immobilise the proteins and indicates that relatively weak electrostatic or hydrophobic interactions are responsible for immobilisation of the protein on the non-ion-activated PS surfaces.

An FTIR-ATR analysis of protein immobilised on the PS and PAC surfaces showed again that the amount of fusion-protein is significantly greater on the PAC surface (Figure 4).

One of the major functions of fibronectin, in particular the RDG section, is cell binding. To test the efficacy of the PAC surfaces with immobilised protein (i.e., fibronectin) and to investigate the adhesion of the cells, rat mesenchymal stem cells (rMSC) were seeded and cultured for 2 and 5 h, their cytoskeleton and nuclei were stained and the cell number was counted. An adhesion assay with cell counting does not directly represent viability or vitality of cells; however it provides information on the number of cells attached to the substrate. It was found that the number of cells that adhered to the surfaces was higher on surfaces with fibronectin than on control samples (PS or PAC only) and fibronectin immobilised on PAC was much more effective than that adsorbed to the bare nickel titanium surface or non-activated PS. The number was significantly greater for the PAC surfaces functionalised with fibronectin (**Figure 5**) which proved that the combination of advanced functional surfaces and fibronectin is highly effective in regulating cell attachment.

Furthermore, an increase in the number of cells attached to the surface (statistically significant) when compared with control samples was observed for fibronectin and fusion-protein coated PAC, and for fusion-protein coated PS samples (Figure 5). The same three groups of samples had significantly

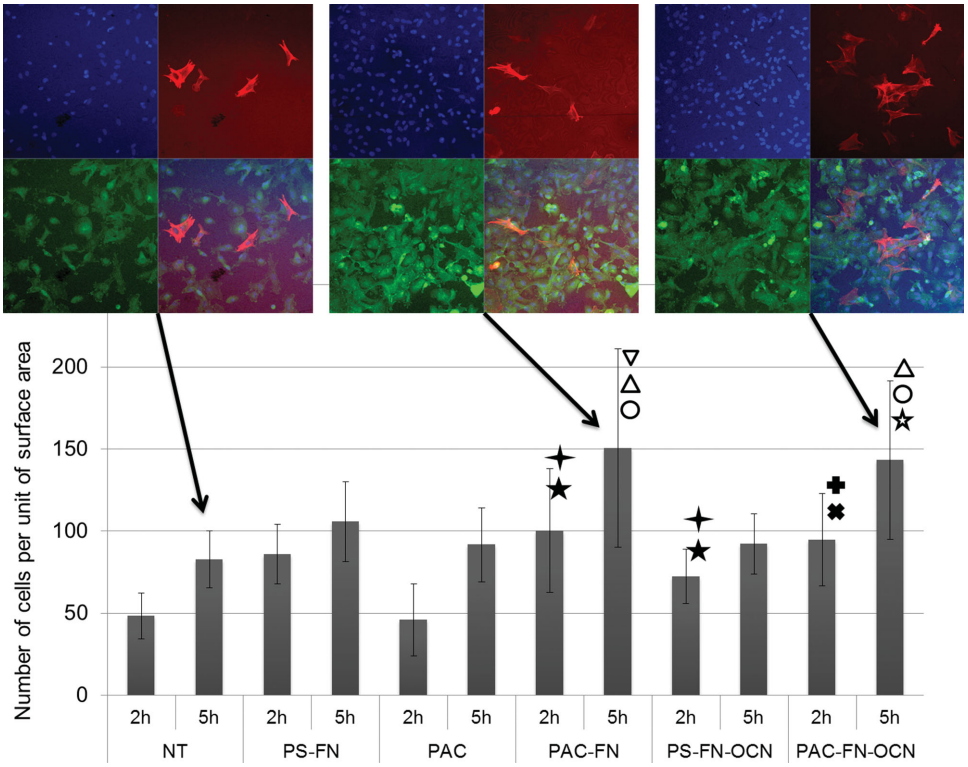

Figure 5. Number of mesenchymal stem cells adhered after 2 and 5 h to control samples and ion-activated PAC samples with and without proteins (FN and FN-OCN); êP < 0.005 compared with NT 2 h; Ò $P < 0.0005$ compared with NT 2 h; ó $P < 0.005$ when compared with NT 5 h; Â $P < 0.05$ when compared with PS-FN 5 h; ç $P < 0.01$ when compared with PAC 2 h; Ë $P < 0.0005$ when compared with PAC 2 h; △$P < 0.01$ when compared with PAC 5 h; ▽$P < 0.05$ when compared with PS-FN-OSC.

greater amounts of attached cells when compared with PAC only samples after 2 h in culture. Importantly, the number of cells after 5 h in culture was significantly greater on both PAC samples with fibronectin and fusion-protein, when compared with: control samples, PS with fibronectin, and PAC. Furthermore, the number of cells was also greater on PAC-FN when compared with PS-FN-OCN. These results suggest that the number of cells attached to protein modified PAC samples was greater, but that there were no differences between fibronectin and fusion-protein. This is consistent with previous observations with enzymes and other ECM proteins that indicate that proteins immobilised on PAC retain a more native and therefore active conformation than those immobilised on PS.[53]

Fluorescent imaging revealed significant densities of focal adhesions and well-developed cytoskeletons for cells cultured on PAC samples with immobilised fibronectin and fusion-protein (Figure 5,6) in early 2 and 5 h as well as late (21 day) time points. On control samples the number of cells was lower but cells were spread with well-developed cytoskeletons (spread actin fibre structure).

However, the primary aim was to provide multifunctional surfaces that simultaneously enhance cell binding and promote ostoinduction, which is important to regulate the integration of implanted materials for bone augmentation devices in the body. To test the capacity of the surfaces to control cell attachment, differentiation and mineralisation, mesenchymal stem cells were kept in culture until day 21 and then markers of osteoblastic differentiation were studied.

The expression of the key osteogenic marker, osteopontin,[64] was tested qualitatively and quantitatively using immunofluorescence and Q-PCR. The expression of osteopontin was significantly greater on the fusion-protein functionalised PAC samples than on PAC with fibronectin or control (non-activated PS) samples. High levels of osteopontin were evidenced using immunochisotchemistry and Q-PCR measurements (**Figure 6,7**). Further evidence of the differentiation that led to the mineralisation of the matrix was obtained with Alizarin Red staining and elemental analysis. Both experiments demonstrated that cells on fusion-protein coated PAC samples underwent osteoblastic differentiation and formed significant quantities of mineralised matrix (**Figure 8**). SEM observations showed that cells on fusion-protein functionalised samples were well-spread, grew densely and had well-developed (mature) morphology (Figure 8). Elemental analysis showed the presence of calcium within the measured cell area, which indicates mineralised matrix. In contrast, cells on both PS and PAC-FN samples were not as well developed and were flattened with thin protrusions radiating from the cells (Figure 8). Elemental analysis did not show any significant amount of calcium in these two groups of samples, in agreement with the other tests suggesting that mineralisation was limited for these two groups of samples.

Together, the measurements of OPN at gene level and of subsequent mineralisation by the Alizarin-Red assay and EDS elemental analysis provide evidence that the stem cells underwent osteoblastic differentiation. These phenomena were observed

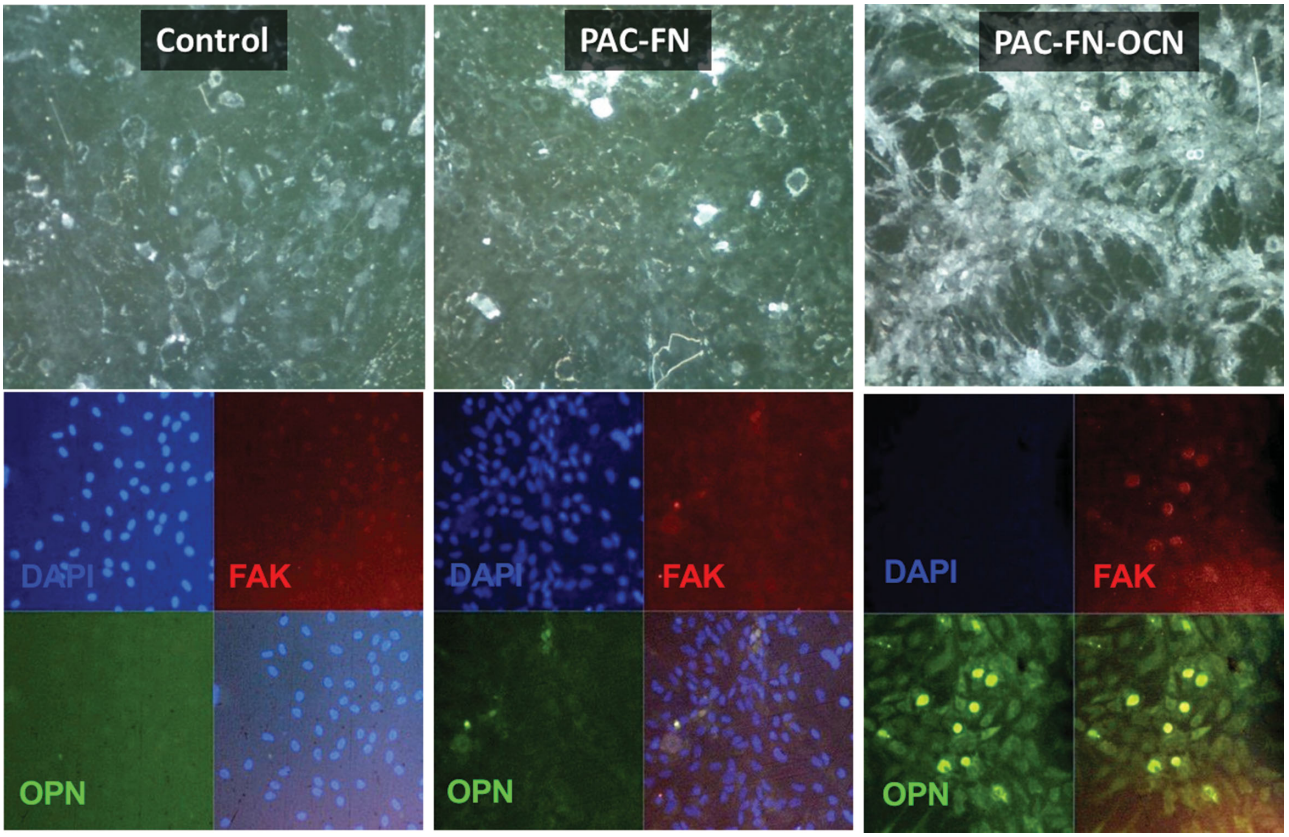

Figure 6. Phase contract and immunostaining images for samples after 21 days in culture for control (bare nickel-titanium), fibronectin immobilised on PAC, and fusion-protein immobilised PAC samples. Fusion protein immobilised samples showed significantly greater density of cells (top row; light microscopy, phase contrast) on the PAC fusion-protein surface. The expression (fluorescent microscopy, bottom row) of both focal adhesions (FAK) and osteopontin (OPN) was evidenced suggesting ostoblastic differentiation of the cells.

for samples functionalised with the fusion-protein, while for non-functionalised control samples and samples functionalised with fibronectin only a negligible amount of OPN and mineralisation were detected.

The above experiments were conducted under osteogenic conditions. The high osteopontin expression with subsequent mineralisation observed for PAC-FN-OCN samples, compared with PAC-FN and control samples, demonstrates that differentiation was modulated primarily by the surface bound fusion-protein. In fact, differentiation and mineralisation was dominated by surface related modulation. Surface functionalisation significantly dominated the effects of the media, which induced negligible mineralisation on control samples. This finding confirms the osteogenic potential of the PAC-FN-OCN surfaces.

These experiments show for the first time that fusion-protein immobilised on a PAC surface is capable of regulating cell adhesion and triggering and modulating osteoblastic differentiation. Hence, fusion-proteins tethered in a desired configuration on the surface of orthopaedic implants through the PAC interface is multifunctional.

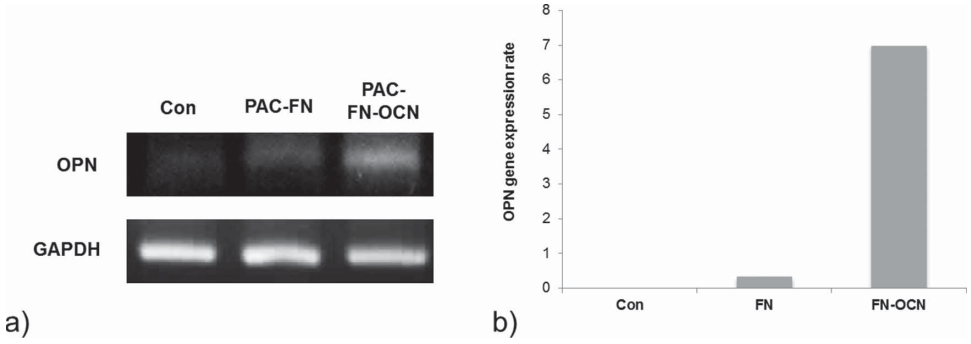

Figure 7. Expression of osteopontin for control nickel titanium (CON), fibronectin immobilised PAC (FN) and fusion-protein immobilised PAC (FN-OCN) measured using a) qualitative and b) and quantitative Q-PCR analysis.

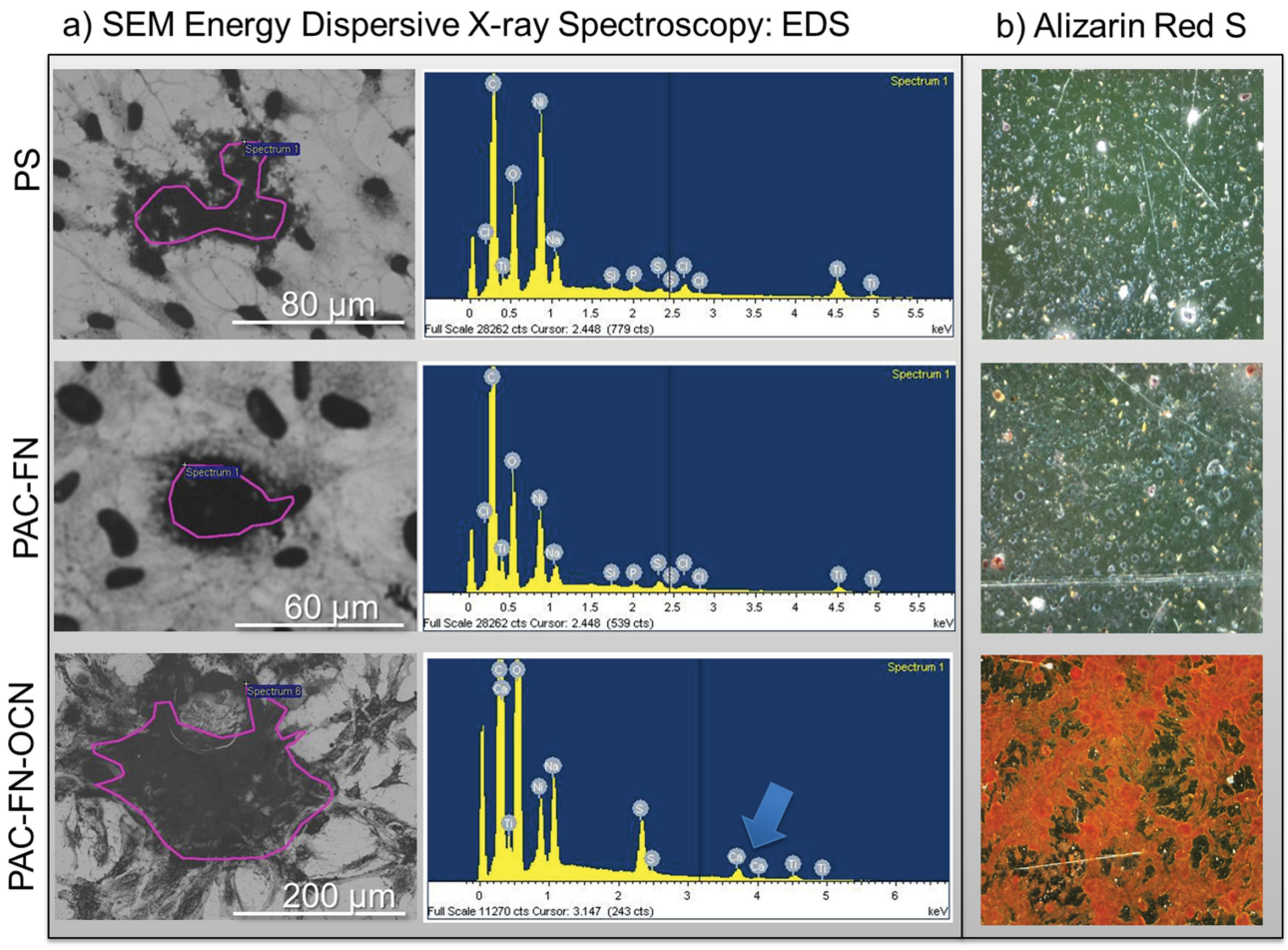

Figure 8. Morphology and mineralisation of the cells after 21 days in culture for control PS and PAC with fibronectin FN, and with fusion protein FN-OCN, showing SEM-EDS and Alizarin Red staining results: a) SEM micrographs of cells with corresponding elemental composition obtained using EDS; b) light microscopy images of samples stained with Alizarin Red dye. Deposition of the calcium (blue arrow) and significant amount of red dyed cells on PAC-FN-OCN samples indicate a significant level of mineralisation. In comparison, limited mineral phase content was observed for PS and PAC-FN samples.

3. Conclusion

The search for a technology that can reduce the side-effects associated with implant integration, while increasing the beneficial effects of the treatment is one of the key targets in biomedical sciences, and this was the primary objective of this study. Life expectancy improved from 49.2 years a century ago to over 78 years now and an ageing population significantly increases the demand for orthopaedic implants.[1,6,11,65–68] It is estimated that annually at least 3.1 million people undergo implantation of an exogenous material or device.[5,68,69] The global biomaterials/medical devices market is estimated at $150 billion,[5,45,70] and metallic implants that include joint endoprosthesis, fracture management devices and dental implants comprise around 10% of the market.[5,70] However, the use of implantable devices is accompanied by the risk of failure, which occurs due to biological incompatibility, infections, wear and loosening.[1,2,4,7,41,71,72] Overall 8.2% and 17.5% of hip and knee implants require replacement leading to substantial costs, disability, and patient productivity loss and discomfort.[5,8,11,65–68] Any advances that minimise adverse reactions through improved implant integration within the body are of great significance and an economical imperative. In this study, we have demonstrated a single step technology that activates the implant material surface via the formation of highly reactive radicals (unpaired electrons) embedded in the surface, enabling it to immobilise bio-molecules in correct orientations and high density. Using this technique to covalently tether novel bi-functional proteins, we have successfully regulated mesenchymal stem cell adhesion and differentiation at the surface. The biointerfaces developed were shown to be capable of triggering and controlling osteoblastic differentiation, and thus osteogenic surfaces were obtained. This technology, in contrast to many nanofabrication approaches, is applicable to complex geometries and can be used easily on large surfaces. An important feature is that topography of the surface does not affect protein adhesion and conformation, which is a significant benefit of this approach and implies that topography, might be tailored separately to give optimal results.

4. Experimental Section

Substrate: Superelastic NiTi alloy (Johnson Matthey Inc. UK) was used in this study. Samples were cut into square shapes of 8 mm × 8 mm and the surface was polished to a mirror finish using SiC paper (grit 500–2400). Prior to surface modification, surfaces were cleaned using a previously published procedure.[72] In brief, samples were first ultrasonicated in isopropyl alcohol, then in deionised water (18 MΩ/cm) for 5 min each and then immersed in nitric acid (63%) for 10 min followed by a final ultrasonication in deionised water for 5 min. Samples were dried with pressurised air. Cleaned NiTi samples (coded as NT) were used as controls.

Polymer Coating: Metal samples were polymer coated with 2% polystyrene solution using a spin coater SCS G3P-8. The thicknesses and optical constants of the spun polymer films, before and after exposure to the plasma, were determined using a spectroscopic ellipsometer (Woollam M2000V). Ellipsometric data were collected for three angles of incidence: 65°, 70°, and 75°. A model consisting of a Cauchy layer on top of a silicon substrate was used to fit the data of untreated PS. The thickness and optical constants associated with the best fit model were determined for each PS layer. The thickness of the spun PS coating measured with ellipsometry was 9.00 ± 0.05 nm. The refractive index was 1.47–1.54 in the 600–800 nm wavelength region. Structural transformations of the interface after PIII treatment change significantly the refractive index of the coating. For this reason three angles (65, 70, and 75 degrees) were used for the ellipsometry measurements. Fitting of all three curves in the 600–800 nm wavelength range gives unique values for refractive index and thickness. The fitting model was verified for stability by varying the starting parameters, checking the matrix of correlation coefficients, variation of wavenumber range, and statistics of the measurement. The model showed high stability of fitting giving confidence that the data determined are physical. The thickness of the PIII treated PS coated samples measured with ellipsometry was 4.7 ± 0.7 nm. A refractive index of 1.98–2.05 in the 600–800 nm wavelength region was assumed based on previous experiments.[39,73,74]

Surface Activation—Nitrogen Plasma Immersion Ion Implantation (PIII): Polystyrene coated samples were modified using ion implantation. The polymer acts as a precursor to produce a highly reactive interface. Nitrogen plasma immersion ion implantation was performed using a PIII system as described in.[39,73] Ions were implanted at the working pressure of 2×10^{-3} Torr; the forward power and reflected powers were 100 W and 12 W respectively; high voltage pulse bias of 20 kV for 20 μs duration at a frequency of 50 Hz was applied to the samples. The voltage was selected to achieve penetration of ions through the PS coating to enhance adhesion of the PS layer to the metal. The ion fluence was calculated to be 20×10^{15} ions cm^{-2} after a treatment time of 800 s. Plasma activated samples were coded as PAC.

Construction and Purification of Fusion Protein (hOC-FN9–10): To construct human osteocalcin (hOC)-FN9–10, the hOCN sequence was initially amplified by the hOCN forward primer (5′-TAGGAGCCCTCACACTCCTC-3), and the hOCN reverse primer (5′-CTGGAGAGGAGCAGAACTGG-3′). In the case of hOC-FN9–10, the restriction site of the hOCN was generated by the forward primer (for BglII site, 5′-AACAGATCTTACCTGTATCAATGGCTGGGA-3), and the reverse primer (for KpnI site, 5′-AATGGTACCGACCGGGCCGTAGAAGCGCCG-3′). In the case of the hOCN-FN9–14, FN9–14 sequence was amplified by the forward primer 5′-ATTGATTATTTGCACGGCGT-3′ and the reverse primer 5′-ACGGCGTTTCACTTCTGAGT-3′. PCR was conducted with PCR mixes over 30 cycles, 1 min at 55 °C for annealing; 1 min at 72 °C for extension, and 1 min at 94 °C for denaturation. Amplified PCR products were digested with BglII, KpnI and KpnI, HindIII. After ligation into pBAD-HisB-FN9–10, pBAD-HisB-hOC-FN9–10 constructs were produced. TOP10 E. coli were grown in LB medium containing ampicilin overnight at 37 °C after transformation. When the absorbance of cultures reached 0.6 (A600), induction was initiated with 0.1% (w/v) L-arabinose and incubated at 20 °C for 6 h. Bacteria were pelleted by centrifugation at 6000*g* for 10 min, lysed, and sonicated. A soluble extract was prepared by centrifugation for 30 min at 14 000*g* in a refrigerated centrifuge and the supernatant was purified by affinity to a nickel-nitrilotriacetic acid resin (Invitrogen, Carlsbad, CA, USA). The purity of recombinant hOCN-FN9–10 and hOCN-FN9–14 was examined under denaturing conditions by Coomassie Brilliant Blue staining of 12% (v/v) sodium dodecyl sulfate-polyacrylamide gel electrophoresis (SDS-PAGE) gel.

Qualitative and Quantitative Analysis of the Protein Immobilisation on the Surface: The surface chemistry of the samples before and after modifications was examined using X-ray photoelectron spectroscopy (XPS, SPECS-XPS, Germany) utilising an Al Kα monochromated X-ray source. A survey scan for each sample was obtained at 100 eV pass energy between 0 and 1400 eV. Five scans were collected for each sample. High resolution spectra for the single elements (C, O, N, Ni, Ti) were recorded at 20 to 50 eV pass energy. The elemental composition (atomic concentration) was calculated from the high-resolution scans using CasaXPS (Casa software Ltd.) after subtracting Shirley background. Evaluation was done on triplicate samples. Surface chemistry was assessed for: nickel-titanium (NT), polystyrene coated nickel-titanium (PS) and polystyrene coated and plasma activated nickel-titanium (PAC) samples. To assess the capability of the surface to immobilise both proteins, samples were incubated for 24 h in fibronectin or fusion-protein solution; 20 μg/mL in 1×10^{-2} M phosphate buffered saline (PBS) at pH 7. After incubation, samples were washed 3 times with PBS and deionised water and surface chemistry was assessed by XPS, while topography was assessed using atomic force microscopy (AsylumResearch, MFP-3D-Bio) operated in AC mode. Spectra and topographical images were recorded before and after incubation with the fibronectin (FN) and with the fusion-protein (FN-OCN) for both PS and PAC samples (PS, PAC, PS-FN, PS FN-OCN, PAC-FN, PAC-FN-OSC). Next, to investigate the ability of the surface to covalently bind the proteins, samples were cleaned using sodium dodecyl sulphate (SDS). SDS is a detergent capable of disrupting noncovalent interactions and removes weakly attached proteins from the surface. Samples were placed in vials containing 15 mL 5% SDS and kept in a water bath at 100 °C for 1 h. Next, the samples were transferred into a container containing 40 mL of deionised water and rinsed. This approach allowed removal of non-covalently bound protein, hence determining the capability of the surface to bind proteins covalently. Both XPS and AFM investigations were conducted for the same groups of samples after subsequent washing with sodium dodecyl sulphate (SDS; coded PS-FN-SDS, PS-FN-OCN-SDS, PAC-FN-SDS, PAC-FN-OSC-SDS).

Quantification of the Adsorption and Orientation of Proteins (Quartz Crystal Microbalance, QCM-D): Quantification of protein adsorption onto the surfaces was determined by quartz crystal microbalance (Q Sense, AB Sweden) with dissipation monitoring (QCM-D). The QCM-D measures frequency (f) and dissipation (*D*) at the fundamental frequency (5 MHz) and three successive overtones (15, 25, and 35 MHz). Experiments were performed at 37 °C. A stable measurement in phosphate buffered saline (PBS) pH 7.2 was established before the addition of protein solutions (50 μg/mL) for 100 min followed by two rinses with PBS.

Determination of the Protein Conformation on the Surface using Fourier Transform Spectroscopy in Attenuated Total Reflectance mode (FTIR-ATR): FTIR-ATR spectra from the samples were recorded using a Digilab FTS7000 FTIR spectrometer (Holliston, MA, USA) fitted with an ATR accessory (Harrick, Pleasantville, NY, USA) with trapezium germanium crystal and incidence angle of 45°. To obtain sufficient signal/noise ratio and resolution of spectral bands we used 500 scans and a resolution of 1 cm^{-1}. All spectral analyses were undertaken using GRAMS software (ThermoFisher, Waltham, MA, USA). Before recording spectra, the surfaces of the samples were dried using dry air. Spectral subtraction was used to obtain differences between spectra of samples before and after treatment to detect changes associated with the surface treatment and subsequent attachment of protein. To determine sodium dodecyl sulfate (SDS) resistant protein binding, samples with attached protein were washed in 5% SDS detergent at 100 °C for 10 min and then washed with de-ionised water three times to remove the residual SDS. FTIR-ATR spectra were recorded before and after the SDS treatment and the difference spectra of protein-incubated samples and buffer-incubated samples (exposed to otherwise identical process steps) determined.

Determination of the Distribution and Presence of the Proteins on the Surface using Molecular Probing: To probe the location and distribution of the proteins an atomic force microscope (MFP-3D-Bio, AsylumResearch) and functionalised silicon-nitride probes (TR800), with nominal spring constant $k = 0.03$ N/m, were used. In the first step, tips were cleaned in piranha solution for 10 min and dried under nitrogen flow. Additionally, probes were cleaned in an ozone cleaner. To attach antibodies (anti-fibronectin) to the tip, probes were coated using chemical vapour deposition with APTES followed by amide coupling. Briefly, tips were purged with nitrogen in a vacuum desicator and a small amount of APTES was placed close to the tips and allowed to evaporate for 12 h. Antibodies were then attached by immersing probes in antibody solution (30 μg/mL) with 10 mM EDC in 5 mM MES buffer for 120 min. After functionalisation the spring constant and sensitivity for each tip were measured using the thermal method. Furthermore, sensitivity of the probes was verified by single indentation into freshly cleaved mica. Functionalised tips were used to probe the location of the proteins by measuring adhesion forces between the tip and the substrate. All the measurements were conducted using freshly prepared samples and probes and the tests were done in PBS. For each sample multiple areas of 1 μm × 1 μm were scanned and for each scan adhesion maps were obtained from 80 × 80 probed points. Force-displacement curves were recorded at a frequency of 0.4 Hz and with maximum deflection of the cantilever (20 nm).

Isolation and Culture of Rat Bone Marrow Mesenchymal Stem Cells (rMSCs): rMSCs were isolated from the bone marrow of tibia and femora of adult Sprague-Dawley rats. All protocols involving animals were conducted according to the guidelines approved by the Animal Ethics Committee of Dankook University. Rats were sacrificed by decapitation, after which the bone marrow was aspirated from the tibiae and femora into Hank's Balanced Salt Solution (HBSS; Gibco, Franklin Lakes, NJ) containing 0.1% collagenase Type I and 0.2% dispase II, and the mononuclear cells were then obtained using the enzyme solution in conjunction with centrifugation at 1500 rpm. Next, the cells were plated at a density of 2×10^3 cells/cm^2 in two parallel culture dishes (one for proteomic analysis and the other for subculturing) and cultured in normal growth medium, composed of alpha-Minimal Essential Medium (alpha-MEM; WelGene, DaeGu, Korea) supplemented with 10% fetal bovine serum (FBS; Hyclone, Logan UT), 2 mM l-glutamine, 100 U/mL penicillin, and 100 mL/mL streptomycin (all from Sigma-Aldrich; St. Louis, MO) at 37 °C in a humidified atmosphere containing 5% CO_2 for 7 days. Cells subcultured for 2–3 passages were used for experiments.

Evaluation of rMSC Adhesion: Cultured rMSCs were harvested by trypsinisation, washed and re-suspended in growth medium. Cells were then seeded on the samples at a density of 5×10^4 cells/cm^2 and incubated for 2 and 5 h to allow cell adhesion. To assess the amount of the cells successfully adhered to the surface at each time point, samples were washed with PBS and fixed with 4% PFA for 5 min at room temperature. Cells were then permeabilised by treating with 0.1% Triton X100 in PBS for 10 min. Samples were incubated with primary antibody solution (rabbit anti-focal adhesion kinase antibody; A-17; 1:100 dilution; Santa Cruz Biotechnology, Santa Cruz, CA) overnight at 4 °C. After washing with PBS, the cells were incubated in fluorescein isothiocynate (FITC)-labelled secondary antibody mixed with phalloidin (A34055, Alexa Fluor 555 phalloidin) for 1 h at room temperature to stain for F-actin. The nuclei were stained with 4,6-diamidino-2-phenylindole (DAPI). After washing with PBS, samples were mounted with anti-fade solution and then analysed using a LSM700 confocal microscope (Carl Zeiss, Germany).

Evaluation of Cell Differentiation based on RT-PCR Analysis of Gene Expression: After culturing for 21 days, cells were harvested by trypsinisation, washed, pelleted by centrifugation and used to analyse the presence and amount of osteogenic protein marker (osteopontin). Total RNA was isolated from each cell pellet using an RNeasy mini kit 74104 (RNA isolation kit, Qiagen, Valencia, CA). RNA samples (1 μg) were reverse transcribed to cDNA in 40 μL using the Quantitect RT kit (Qiagen) according to the manufacturer's protocol. The reaction was allowed to proceed at 95 °C for 5 min. A similar reaction mixture without the reverse transcriptase enzyme was prepared and used as a template to demonstrate the absence of contaminating genomic DNA. One microliter of cDNA was subjected to PCR amplification using specific primers for rat osteopontin (OPN) with a pre-mixed PCR kit (Bioneer, Daejon, Korea). PCR reactions were conducted using 40 cycles at 95 °C for 30 s, 55 °C for 30 s, and 75 °C for 60 s, and were performed in triplicate for each cDNA. Sample band intensity was quantified using a Gene tools software program (Gene tools v. 4.01, Syngene, UK) and normalised to that of endogenous GAPDH transcripts.

Evaluation of Cell Differentiation based on Immunocytochemical Analysis of Bone-Specific Protein Expression: rMSCs were cultured on PS and PAC samples with immobilised FN and FN-OCN. Cells were grown for 21 days in the presence of osteogenic growth medium containing 10 mM alpha-glycerophosphate, 50 μg/mL ascorbic acid and 10 nM dexamethasone. For immunocytochemistry, samples were fixed with 4% PFA solution for 5 min and then washed three times with PBS. Cell were permeabilised with 0.1% Triton-X100 in PBS solution for 10 min. Samples were incubated with mouse anti-OPN antibody (1:100; SC73631; Santa Cruz Biotechnology) overnight at 4 °C. Samples were then washed three times with PBS and incubated with FITC-conjugated anti-mouse secondary antibody (1:500, A11001; Invitrogen) for 1 h at room temperature. Images were analysed using confocal microscopy (LSM700 microscope, Carl Zeiss).

Alizarin Red S Staining for Mineralisation Assay: To assess the level of the mineralisation each sample was fixed with 2.5% glutaraldehyde and stained using Alizarin Red S (ARS) dye (mineralisation assay). ARS is a dye that binds calcium salts selectively and is widely used as a bone histochemical marker for assessing bone maturation and mineralisation. 1% ARS, adjusted to pH 4.1–4.3 with 0.5% ammonium hydroxide was prepared and samples were washed three times in PBS and incubated with the ARS solution for 30 min. Next, samples were washed several times with ultra-pure water and viewed using an optical microscope (Olympus Eclipse Ti-U).

Assessment of the Mineralisation using Elemental Analysis (SEM-EDX): Scanning electron microscopy (Bruker, SNE-3000M) and elemental analysis (energy dispersive spectroscopy) were used to assess cell morphology and measure the level of mineralisation after 21 days in culture. Cells were fixed using 2.5% glutaraldehyde, dehydrated in an alcohol series, mounted on SEM stubs and then Pt coated. Micrographs of the samples were recorded, while the level of mineralisation was assessed based on the presence of calcium, averaged over selected cell surface areas.

Statistical Analysis: Data are presented as the mean ± one standard deviation. Statistical comparisons were made using two tailed Student *t*-tests. Statistical significance was considered at different levels ($P < 0.05$, $P < 0.01$, $P < 0.005$, $P < 0.0005$).

Supporting Information

Supporting Information is available from the Wiley Online Library or from the author.

Acknowledgements

Marcela Bilek gratefully acknowledges financial support from the Australian Research Council in the form of project grant funding and salary support from a Future Fellowship. Alexey Kondyurin was in part supported from the International Research Group Program, Perm region Government. This study was supported by grants from the Priority Research Centers Program (2009-0093829), National Research Foundation, Republic of Korea. Authors gratefully acknowledges Steven Devenish for help with AFM tips functionalisation

Received: May 26, 2014
Revised: July 13, 2014
Published online: September 30, 2014

[1] B. D. Ratner, *Polymer International* **2007**, *56*, 1183–5.
[2] L. Y. Liu, G. Chen, T. Chao, B. D. Ratner, E. H. Sage, S. Y. Jiang, *Journal of Biomaterials Science-Polymer Edition* **2008**, *19*, 821–35.
[3] B. D. Ratner, S. J. Bryant, *Annual Review of Biomedical Engineering* **2004**, *6*, 41–75.
[4] B. D. Ratner, *Biomaterials science: An introduction to materials in medicine* **2004**, xi+484p.
[5] V. Antoci, J. Parvizi, in *Comprehensive Biomaterials*, Elsevier, Oxford **2011**, pp 109–26.
[6] V. Antoci, C. S. Adams, J. Parvizi, H. M. Davidson, R. J. Composto, T. A. Freeman, E. Wickstrom, P. Ducheyne, D. Jungkind, I. M. Shapiro, N. J. Hickok, *Biomaterials* **2008**, *29*, 4684–90.
[7] B. D. Ratner, *Biomaterials science: An introduction to materials in medicine* **2004**, 465–71.
[8] J. M. Anderson, B. Bevacqua, A. N. Cranin, L. M. Graham, A. S. Hoffman, M. Klein, J. B. Kowalski, R. F. Morrissey, S. A. Obstbaum, B. D. Ratner, F. J. Schoen, A. Sirakian, D. Whittlesey, *Biomaterials science: An introduction to materials in medicine* **2004**, 415–55.
[9] R. G. Richards, Introduction: Implants and infection in fracture fixation "ten years on". Injury **2006**, *37*, S1-S2.
[10] R. G. Richards, *Eur Cell Mater* **2008**, *16*, 9.
[11] J. M. Anderson, A. Rodriguez, D. T. Chang, *Seminars in Immunology* **2008**, *20*, 86–100.
[12] D. F. Williams, *Biomaterials* **2008**, *29*, 2941–53.
[13] Statistics ABo. 1301.0 – Year Book Australia, 2009–10 Canberra: Australian Bureau of Statistics **2010**.
[14] T. Sjöström, M. J. Dalby, A. Hart, R. Tare, R. O. C. Oreffo, B. Su, *Acta Biomaterialia* **2009**, *5*, 1433–41.
[15] M. J. P. Biggs, R. G. Richards, S. McFarlane, C. D. W. Wilkinson, R. O. C. Oreffo, M. J. Dalby, *Journal of the Royal Society Interface* **2008**, *5*, 1231–42.
[16] M. J. Dalby, N. Gadegaard, R. Tare, A. Andar, M. O. Riehle, P. Herzyk, C. D. W. Wilkinson, R. O. C. Oreffo, *Nature Materials.* **2007**, *6*, 997–1003.
[17] W. Chrzanowski, A. Kondyurin, J. H. Lee, M. S. Lord, M. M. Bilek, H. W. Kim, *J Mater Sci Mater Med* **2012**, *23*, 2203–15.
[18] M. S. Lord, C. Modin, M. Foss, M. Duch, A. Simmons, F. S. Pedersen, B. K. Milthorpe, F. Besenbacher, *Biomaterials* **2006**, *27*, 4529–37.
[19] W. Chrzanowski, E. A. Abou Neel, K. Y. Lee, A. Bismarck, A. M. Young, A. D. Hart, M. J. Dalby, J. C. Knowles, *Advanced Engineering Materials* **2010**, *12*, B298–B308.
[20] W. Chrzanowski, D. A. Armitage, J. C. Knowles, J. Szade, W. Korlacki, J. Marciniak, *Journal of Biomaterials Applications* **2008**, *23*, 51–71.
[21] W. Chrzanowski, E. A. bou Neel, D. A. Armitage, K. Lee, W. Walke, J. C. Knowles, *Journal of the Royal Society Interface* **2008**, *5*, 1009–22.
[22] M. J. Dalby, S. Childs, M. O. Riehle, H. J. H. Johnstone, S. Affrossman, A. S. G. Curtis, *Biomaterials* **2003**, *24*, 927–35.
[23] M. J. Dalby, D. Giannaras, M. O. Riehle, N. Gadegaard, S. Affrossman, A. S. G. Curtis, *Biomaterials* **2004**, *25*, 77–83.
[24] M. J. Dalby, D. McCloy, M. Robertson, H. Agheli, D. Sutherland, S. Affrossman, R. O. C. Oreffo, *Biomaterials* **2006**, *27*, 2980–7.
[25] R. J. McMurray, N. Gadegaard, P. M. Tsimbouri, K. V. Burgess, L. E. McNamara, R. Tare, K. Murawski, E. Kingham, R. O. C. Oreffo, M. J. Dalby, *Nat Mater* **2011**, *10*, 637–44.
[26] L. E. McNamara, M. O. Riehle, M. J. Dalby, R. Burchmore, *Tissue Engineering* **2007**, *13*, 175.
[27] G. McPhee, M. Dalby, M. Riehle, H. Yin, *Medical and Biological Engineering and Computing* **2010**, *48*, 1043–53.
[28] J. Y. Lim, H. J. Donahue, *Tissue Engineering* **2007**, *13*, 1879–91.
[29] N. Mitchell, R. Schlapak, M. Kastner, D. Armitage, W. Chrzanowski, J. Riener, P. Hinterdorfer, A. Ebner, S. Howorka, *Angewandte Chemie-International Edition* **2009**, *48*, 525–7.
[30] R. Schlapak, D. Armitage, N Saucedo-Zeni, W. Chrzanowski, M. Hohage, D. Caruana, S. Howorka, *Soft Matter* **2009**, *5*, 613–21.
[31] S. K. Misra, S. E. Philip, W. Chrzanowski, S. N. Nazhat, I. Roy, J. C. Knowles, V. Salih, A. R. Boccaccini, *Journal of the Royal Society Interface* **2009**, *6*, 401–9.
[32] P. Roach, D. Farrar, C. C. Perry, *Journal of the American Chemical Society* **2006**, *128*, 3939–45.
[33] P. Roach, T. Parker, N. Gadegaard, M. R. Alexander, *Surface Science Reports* **2010**, *65*, 145–73.
[34] M. S. Lord, M. Foss, F Besenbacher, *Nano Today* **2010**, *5*, 66–78.
[35] R. G. LeBaron, K. A. Athanasiou, *Tissue Engineering* **2000**, *6*, 85–103.
[36] C. Yongli, Z. Xiufang, G. Yandao, Z. Nanming, Z. Tingying, S Xinqi, *Journal of Colloid and Interface Science* **1999**, *214*, 38–45.
[37] S. K. Zareh, Y. M. Wang, *Microscopy Research and Technique* **2011**, *74*, 682–7.
[38] K. Lee, R. R. Itharaju, D. A. Puleo, *Acta Biomaterialia* **2007**, *3*, 515–22.
[39] M. M. M. Bilek, D. V. Bax, A. Kondyurin, Y. Yin, N. J. Nosworthy, K. Fisher, A. Waterhouse, A. S. Weiss, C. G. dos Remedios, D. R. McKenzie, *Proceedings of the National Academy of Sciences* **2011**, *108*, 14405–10.
[40] A. Wilz, E. M. Pritchard, T. Li, J. Q. Lan, D. L. Kaplan, D Boison, *Society for Neuroscience Abstract Viewer and Itinerary Planner* **2008**, *38*.
[41] I. Ahmed, D. Ready, M. Wilson, J. C. Knowles, *Journal of Biomedical Materials Research Part A* **2006**, *79A*, 618–26.
[42] F. Rehfeldt, A. J. Engler, A. Eckhardt, F. Ahmed, D. E. Discher, *Advanced Drug Delivery Reviews* **2007**, *59*, 1329–39.
[43] C. Garcia, S. Cere, A Duran, *Journal of Non-Crystalline Solids* **2006**, *352*, 3488–95.
[44] T. Xi, R. Gao, B. Xu, L. Chen, T. Luo, J. Liu, et al. *Biomaterials* **2010**, *31*, 5151–8.
[45] N. J. Hickok, C. Ketonis, C. S. Adams, in *Comprehensive Biomaterials*, Elsevier, Oxford **2011**, pp 281–94.
[46] E. Birmingham, G. L. Niebur, P. E. McHugh, G. Shaw, F. P. Barry, L. M. McNamara, *Eur Cell Mater* **2012**, *23*, 13–27.
[47] J. N. Beresford, J. A. Gallagher, J. W. Poser, R. G. G. Russell, *Metabolic Bone Disease and Related Research* **1984**, *5*, 229–34.
[48] D. Laurencin, N Almora-Barrios, N. H. de Leeuw, C. Gervais, C. Bonhomme, F. Mauri, W. Chrzanowski, J. C. Knowles, R. J. Newport, A. Wong, Z. Gan, M. E. Smith, *Biomaterials* **2011**, *32*, 1826–37.
[49] N. K. Lee, H. Sowa, E. Hinoi, M. Ferron, J. D. Ahn, C. Confavreux, R. Dacquin, P. J. Mee, M. D. McKee, D. Y. Jung, Z. Zhang, J. K. Kim, F. Mauvais-Jarvis, P. Ducy, G. Karsenty, *Cell* **2007**, *130*, 456–69.
[50] M. Ahmad, M. McCarthy, G Gronowicz, *Biomaterials* **1999**, *20*, 211–20.
[51] R. T. Franceschi, B. S. Iyer, *Journal of Bone and Mineral Research* **1992**, *7*, 235–46.
[52] W. Chrzanowski, S. P. Valappil, C. W. Dunnill, E. A. Abou Neel, K. Lee, I. P. Parkin, M. Wilson, D. A. Armitage, J. C. Knowles, *Materials Science and Engineering: C* **2010**, *30*, 225–34.
[53] W. Chrzanowski, I. Raizer, N. Mordan, J. C. Knowles, V Salih, *eCM – European Cells and Materilas* **2012**, *23*, 63.
[54] E. A. Kosobrodova, A. V. Kondyurin, K. Fisher, W. Moeller, D. R. McKenzie, M. M. M. Bilek, *Nuclear Instruments and Methods in Physics Research Section B: Beam Interactions with Materials and Atoms* **2012**, *280*, 26–35.
[55] A. Kondyurin, P. Naseri, K. Fisher, D. R. McKenzie, M. M. M. Bilek, *Polymer Degradation and Stability* **2009**, *94*, 638–46.
[56] A. Kondyurin, N. J. Nosworthy, M. M. Bilek, *Langmuir* **2011**, *27*, 6138–48.
[57] B. K. Gan, A. Kondyurin, M. M. Bilek, *Langmuir* **2007**, *23*, 2741–6.

[58] F. Höök, J. Vörös, M. Rodahl, R. Kurrat, P Böni, J. J. Ramsden, M. Textor, N. D. Spencer, P. Tengvall, J. Gold, B. Kasemo, *Colloids and Surfaces B: Biointerfaces* **2002**, *24*, 155–70.
[59] J. B. Lhoest, E. Detrait, P. van den Bosch de Aguilar, P. Bertrand, *Journal of Biomedical Materials Research* **1998**, *41*, 95–103.
[60] V. E. Koteliansky, M. A. Glukhova, M. V. Benjamin, V. N. Smirnov, V. V. Filimonov, O. M. Zalite, S. Venyaminov, *European Journal of Biochemistry* **1981**, *119*, 619–24.
[61] A. J. Lee, S. Hodges, R Eastell, *Ann Clin Biochem* **2000**, *37*, 432–46.
[62] Y. Yin, M. M. M. Bilek, D. R. McKenzie, N. J. Nosworthy, A. Kondyurin, H. Youssef, M. J. Byrom, W. Yang, *Surface and Coatings Technology* **2009**, *203*, 1310–6.
[63] M. Bilek, D McKenzie, *Biophys Rev* **2010**, *2*, 55–65.
[64] Q.-Z. Chen, H. Ishii, G. A. Thouas, A. R. Lyon, J. S. Wright, J. J. Blaker, W. Chrzanowski, A. R. Boccaccini, N. N. Ali, J. C. Knowles, S. E. Harding, *Biomaterials* **2010**, *31*.
[65] Y.-M. Lin, W. Chrzanowski, J. Knowles, A. Bishop, A Bismarck, *Advanced Engineering Materials* **2010**, *12*, B101–B12.
[66] Y. Oshida, in *Bioscience and Bioengineering of Titanium Materials*, Elsevier, Oxford **2007**, pp 157–214.
[67] R. M. Donlan, J. W. Costerton, *Clinical Microbiology Reviews* **2002**, *15*, 167–93.
[68] J. A. Singh, J. A. Kundukulam, M Bhandari, *Pharmacoepidemiol Drug Saf* **2012**, *1*, 265–73.
[69] A. B. Faia-Torres, T. Goren, M. Textor, M Pla-Roca, in *Comprehensive Biomaterials*, Elsevier, Oxford **2011**, pp 181–201.
[70] W. Chrzanowski, E. A. A. Neel, D. A. Armitage, X. Zhao, J. C. Knowles, V Salih, *J Biomed Mater Res A* **2010**, *93*, 1596–608.
[71] E. A. Cavalcanti-Adam, A. Micoulet, J Blümmel, J. Auernheimer, H. Kessler, J. P. Spatz, *European Journal of Cell Biology* **2006**, *85*, 219–24.
[72] E. A. Cavalcanti-Adam, T. Volberg, A. Micoulet, H. Kessler, B. Geiger, J. P. Spatz, *Biophysical Journal* **2007**, *92*, 2964–74.
[73] A. Kondyurin, N. J. Nosworthy, M. M. M. Bilek, *Acta Biomaterialia* **2008**, *4*, 1218–25.
[74] C. T. Tran, A. Kondyurin, W. Chrzanowski, M. M. Bilek, D. R. McKenzie, *Colloids Surf B Biointerfaces* **2013**, *104*, 145–52.